

Unmasking the Therapeutic Potential of a Bio-enhanced Phloretin Formulation: Formulation, Characterization, and Evaluation

Niyamat M.A. Chimthanawala, Purnima D. Amin, Sadhana S. Sathaye*

Department of Pharmaceutical Sciences and Technology, Institute of Chemical Technology, Nathalal Parekh Marg, Matunga, Mumbai, Maharashtra, INDIA.

ABSTRACT

Introduction: Phloretin (PHL, 3-(4-Hydroxyphenyl)-1-(2,4,6-trihydroxyphenyl) propan-1-one), is a naturally occurring dihydrochalcone, exclusively found in apple fruit peels, leaves, and Manchurian apricots. It has tremendous benefits as an antioxidant, anti-inflammatory, neuroprotective and anti-cancer agent but its Bioavailability (BA) and penetration across the Blood-Brain Barrier (BBB) is limited as it is a BCS class II drug, thereby hindering its therapeutic applications. **Materials and Methods:** In this study, we report the formulation, development, and characterization of an Oral Solid Dispersion (ASD) of PHL, designed to enhance its BA and brain distribution, by incorporating non-ionic surfactants like Poloxamer® 188 (P188) and Gelucire® 48/16 (GEL), & excipients like Neusilin® S2 (NEU), in a reproducible, solvent-free approach using melt-fusion technology. Comprehensive characterization included, Differential Scanning Calorimetry (DSC), X-ray Diffraction (XRD), Fourier-Transform Infrared Spectroscopy (FTIR), and Scanning Electron Microscopy (SEM) to compare pure PHL, binary formulations (FPOX: PHL+P188; FGEL: PHL+GEL 48/16), and its Physical Mixtures (PM). *In vitro* drug release (dissolution, solubility, and accelerated stability) with *in vivo* Pharmacokinetic (PK) profiling was carried out to assess improved performance. Bioanalytical validation of an RP-HPLC method was done to analyse the samples. Additionally, *in vitro* antioxidant and anti-inflammatory activities were evaluated. **Results and Discussion:** The optimized formulation, FPOX with the strategic inclusion of P188 and NEU in an ASD had improved physical stability, dissolution rate, and at an equivalent dose of 10 mg/kg, showed enhanced PK parameters as was analysed by a robust, validated HPLC method. It retained its biological efficacy supporting its potential in phytopharmaceuticals.

Keywords: Phloretin, Solid dispersion, Antioxidant, Pharmacokinetics, Melt-fusion.

Correspondence:

Prof. (Dr.) Sadhana S. Sathaye
Pharmacology Lab, Department of
Pharmaceutical Sciences and Technology,
Nathalal Parekh Marg, Matunga,
Mumbai-400019, Maharashtra, INDIA.
Email: niyamataqua@gmail.com,
sadhanasathaye@hotmail.com
ORCID: 0000-0002-8568-0994

Received: 11-12-2025;

Revised: 02-01-2026;

Accepted: 27-02-2026.

INTRODUCTION

Neurodegenerative Diseases (NDs) such as Alzheimer's Disease (AD), Parkinson's disease, Huntington's disease, and others, are a group of complex ailments with a heterogenous predisposition, having certain hallmark features like progressive degeneration of neurons, formation of misfolded proteins, accumulation of toxic species, escalating a cascade of metabolic reactions generating Reactive Oxygen Species (ROS), exacerbating neuroinflammation, and causing mitochondrial damage. With the need for emergent and exclusive therapies, there has been a paradigm shift in healthcare towards a multi-target approach; introducing holistic remedies that can target the cellular

metabolic processes and act as safe therapeutic adjuvants to the classically prescribed medications. Among the rich repository of plant-based remedies, polyphenols are an upcoming class of secondary metabolites that offer tremendous potential in the management of these debilitating conditions.^{1,2}

Polyphenols have gained significant traction in the past decade due to their benefits in the nutraceutical, pharmaceutical, and cosmetic industries.³ As a major group of phytochemicals, with more than 8000 varieties in nature,⁴ and multiple phenolic groups, they possess a unique physicochemical profile. A prime challenge in developing formulations incorporating polyphenols is to counter their limited Bioavailability (BA) and navigate the Blood Brain Barrier (BBB) until it reaches the site of action. They can protect plants from parasites and predators, and against oxidative damage by scavenging free radicals.⁵ This property is most sought in the treatment of NDs. In addition to this, polyphenols also modulate oxidative stress-sensitive signaling pathways by reducing the expression and activation of transcription factors such as nuclear factor- κ B (NF- κ B) and Activator Protein-1 (AP-1),



DOI: 10.5530/ijper.20264165

Copyright Information :

Copyright Author (s) 2026 Distributed under
Creative Commons CC-BY 4.0

Publishing Partner : Manuscript Technomedia. [www.mstechnomedia.com]

which are central to inflammation and neurodegeneration.^{6,7} Their neuroprotective effects are demonstrated by regulating mitochondrial apoptosis, upregulating Bcl-2 and downregulating Bax, thereby stabilizing mitochondrial integrity, preventing cytochrome c release, and reducing caspase activation.⁷⁻⁹

Flavonoids are one such class of polyphenols that are ubiquitous in nature.⁴ Notably present in fruits and vegetables, these phenolic compounds are largely present in apples (*Malus domestica* Borkh.) family – Rosaceae.¹⁰ As the old adage goes, “an apple a day, keeps the doctor away,”¹¹ consumption of apples can benefit humans as they are rich in flavonols like quercetin, dihydrochalcones like Phloretin (PHL), its glucoside derivative Phloridzin (PHZ), and flavan-3-ols like epicatechin, all primarily antioxidants.¹² Although their concentrations vary on the apple variety, they are still effective¹³ in reducing the risk of Cardiovascular (CVS) disease, asthma, some cancers, and diabetes.¹⁴

PHL, also found in strawberries and Manchurian apricots, has been widely studied for its diverse pharmacological properties, including antioxidant, anti-inflammatory, and anti-cancer activities.¹⁵ In CVS disorders, PHL restores Sirtuin 1 (SIRT1) signalling, alleviates myocardial fibrosis, and improves cardiac function; it inhibits aldose reductase and Advanced Glycation End product (AGE) formation and activates the AMP-activated protein kinase (AMPK/SIRT3) pathway in vascular endothelium, reducing mitochondrial ROS via Manganese Superoxide Dismutase (Mn-SOD) deacetylation.¹⁶⁻¹⁸ It offers neuroprotection by preserving mitochondrial membrane potential, reducing ROS and inflammation, limiting lipid peroxidation, thereby improving cognitive performance in AD models.^{19,20} Imparting longevity,²¹ its antioxidant role involves donating a proton H⁺ to free radicals abolishing their reactivity, leading to the formation of a stable flavonoid radical.^{22,23}

Its clinical utility is, however, hindered by poor aqueous solubility, which significantly limits its oral BA. Since it is a Biopharmaceutics Classification System (BCS) class II drug,¹⁵ various formulation strategies have been explored over the past two decades, like Solid Dispersion (SD) with Polyvinylpyrrolidone, PHL-microemulsion for vaginitis treatment,²⁴ hydroxypropyl- β -cyclodextrin using a co-evaporation method,^{25,26} PHL-loaded propylene glycol ethosomes,²⁷ mixed polymeric modified self-nanoemulsions,²⁸ among others, however, they have been met with limited success.

The aim of this study was to formulate a bio-enhanced Amorphous Solid Dispersion (ASD) of PHL with improved BA using polymers like Poloxamer[®] 188 (POX) and Gelucire[®] 48/16 (GEL) by melt-fusion technique. The polymers have low melting points (< 60 °C) making them suitable for ASDs. Further, it was conformed into a consistent, free-flowing powder with Neusilin[®] US2 (NEU), a multi-functional carrier, that protects the active pharmaceutical ingredient (API) from moisture and enhances solubility of poorly soluble APIs. POX is a non-ionic amphiphilic

polyoxyethylene - polyoxypropylene block copolymer beneficial in preventing recrystallization, resulting in stable SDs.²⁹ Although the mechanism is not entirely understood, its bioactivity could be due to its ability to intercalate with the membrane bilayers and increase the density of lipid packing. GEL is a non-ionic surfactant with a unique composition of lipids, surfactants, and co-surfactant built on blocks of Polyethylene Glycol (PEG), that solubilises and boosts the oral BA for lipid-based formulations.³⁰ ASDs can significantly reduce the particle size and enable drug wettability.³¹ Polymers like POX and GEL are 3rd generation SDs intended at achieving the highest degree of BA for poorly soluble drugs like PHL. Lastly, a permeation enhancer, Labrasol[®] ALF (LAB), a non-ionic surfactant (caprylocaproyl polyoxyl-8 glycerides), that has been known for its excellent bio-enhancing abilities in oral drug delivery systems such as Self-Microemulsifying Drug Delivery Systems (SMEDDS/SNEDDS), surfactant-enriched liposomes, and liquid-solid formulations³² was added. The final formulation was characterized, efficacy and release of drug was assessed *in vitro*, followed by *in vivo* Pharmacokinetic (PK) analysis employing a robust and validated Reverse Phase-High Performance Liquid Chromatography (RP-HPLC) method.

MATERIALS AND METHODS

In silico Investigation

For a preliminary investigation into the role and features of the phytochemical, two *in silico* databases that are freely available online were explored; viz. the Comparative Toxicogenomics Database (CTD) <http://ctdbase.org/> and ADMETlab 2.0. CTD is a comprehensive database that defines and correlates associations between chemicals in the environment, and the impact of their exposures on human health. ADMETlab 2.0 is an online software with a highly trained prediction model for the absorption, distribution, metabolism, excretion and toxicity profile of a compound. It reports the physicochemical properties and medicinal chemistry friendliness of the compound.^{33,34} The SMILES format of PHL was uploaded in the software and a detailed report was obtained. <https://admetmesh.scbdd.com/>

Chemicals and Reagents

PHL (API, >98.0%) was procured from Tokyo Chemical Industry Co., Ltd., (Tokyo, Japan). P188, and NEU, (Fuji Chemical Industry Co. Ltd.,) were a gift from BASF India and Gangwal Chemicals, Mumbai, respectively whereas GEL and LAB were gifts from Gattefossé, India (Table S1). Methanol (MeOH), Acetonitrile (ACN), were HPLC grade solvents. Milli-Q (MQ) water was used throughout the experiments (Millipore, Bedford, MA, USA). All the other chemicals for the study were laboratory grade.

Animals

Adult male Sprague-Dawley (SD) rats (250 ± 20 g) were purchased from the National Institute of Biosciences, Pune and

allowed a 1-week acclimatization period before commencing the experiments. They were housed in separate cages under ambient conditions (temperature: $23 \pm 2^\circ\text{C}$; 12 hr light–dark cycle; relative humidity: 50%). Water and food pellets were freely accessible as per their standard diets. Prior to the PK study, rats were kept on fasting for 04 hr with free access to water. Blank plasma was procured from the rats after approval from the Institutional Animal Ethics Committee (IAEC) committee (ICT/IAEC/2022/P03) of the Institute of Chemical Technology (ICT), Mumbai, India in accordance with the Committee for the Control and Supervision of Experiments on Animals (CCSEA).

Optimisation and Formulation

Optimization

Firstly, three different techniques, viz. Solvent Evaporation (SE), Cold-Press (CP), and Melt-Fusion (MF) technique were used to develop an ASD of PHL.³⁵ Secondly, a range of polymers (P188, P407, GEL48/16) were tested for selecting the polymer of choice. The most suitable, reproducible method for developing the formulation was used. All excipients were generally recognized as safe. The methods have been explained in detail in a supplementary file (Table S1).

Formulation

Weighed amount of the polymers (P188 – coarse white powder or GEL48/16 - pellets) were taken in a container on a hot plate and allowed to heat until complete melting. The melting temperature should not exceed 60°C . After the polymer completely melted, and a semi-solid golden mixture was obtained, PHL was added, gradually, till it was completely mixed with the polymers. Then LAB (10%) was added to enhance permeation, on gentle heating with continuous stirring followed by NEU till a free-flowing powder was obtained. A 40-mesh sieve was used to get a uniform ASD. The powders were weighed and stored in air-tight plastic containers at Room Temperature (RT). A ratio of 1:3:0.5:2 was optimized after several trials (Table S2).

Characterization

The API, prepared ASD formulations (FPOX, FGEL), Physical Mixtures (PM_POX, PM_GEL), and corresponding controls – CONT_POX, CONT_GEL were characterized by Scanning Electron Microscopy (SEM), Differential Scanning Calorimetry (DSC), X-ray Diffraction (XRD), and Fourier Transform Infrared (FTIR) spectroscopy studies.

FTIR

FTIR spectroscopy was employed to measure the possible chemical interactions between PHL and the polymer matrix. All the samples were analysed using Jasco FTIR-4600 series spectrophotometer. Samples were prepared in KBr, compressed into discs and analysed in the scanning range from $400\text{--}4000\text{ cm}^{-1}$ at a resolution of 4 cm^{-1} .

DSC

DSC analysis was carried out to monitor possible physical interactions. For thermal characterisation of the samples, a quantity of about 7 mg was placed within open aluminium crimp pans (size: $D6 \times 2.5\text{ mm}$), and subjected to thermal analysis at a scanning rate of $10^\circ\text{C}/\text{min}$ across a temperature spectrum ranging from $30\text{--}250^\circ\text{C}$. Aluminium pans served as the standard reference material for the calibration of both the temperature and energy scales of the DSC apparatus. The thermal behavior was examined under a nitrogen flow of $100\text{ mL}/\text{min}$ on TA Instruments, model SDT Q600.

XRD

The powder XRD diffractograms of all the formulations were recorded using a high-resolution X-ray diffractometer, Rigaku SmartLab, SmartLab Studio II v4.3.152.0 software for analysis. The conditions used to obtain a 1D scan using a standard goniometer were, D/teX Ultra 250 detector, $K\beta$ filter 1D for Cu, 45 kV voltage, current 40 mA, scanning rate of $15^\circ/\text{min}$, and scanning range of $5 \sim 80^\circ$. The diffractograms obtained were plotted in intensity counts (cps) and $2\theta^\circ$ values.

SEM

The morphology of the formulations was examined using SEM type – QUANTA 200 ESEM, ICON Labs, Mumbai with an accelerating voltage of kV:20 resolution:(eV) 129.5. pressure 64 Pa, employing a large field detector. Samples were placed on Aluminium stubs by double-sided adhesive carbon tape and coated using a sputter coater. High resolution images were taken at a range of magnifications (500-4000x). The EDAX APEX software was used to depict the surface morphology and chemical elemental composition.

In vitro Release

Saturation solubility

The saturated solubility of the drug was determined in Distilled Water (DW) and various buffers from pH 1.2 to 7.4. An excess amount of drug was added to 2 mL of DW or buffer of required pH in a microcentrifuge tube (Eppendorf tube). The tubes were kept on an orbital shaker for 48 hr (speed: 50 rpm, temperature: $25 \pm 0.5^\circ\text{C}$). The samples were then filtered (0.22 μm syringe filters), filtrates collected, and absorbance measured with UV-visible Spectrophotometer (UV-1601PC, Shimadzu Corporation, Japan), UV Probe software, on selected λ_{max} for PHL.³⁶ Calibration curves of the different solvents were used to calculate the concentrations. The results were obtained in triplicates and presented as Mean \pm Standard Deviation (SD).

Dissolution

For studying the drug release *in vitro*, dissolution studies for PHL (50 mg) and its SDs equivalent to 50 mg PHL (FPOX and

FGEL) was carried out on USP dissolution apparatus II (basket type) with paddles (LABINDIA® DS8000, India), in a dissolution media of 900 mL gastric fluid without enzymes (pH=1.2) at $37 \pm 0.5^\circ\text{C}$ and speed of 75 rpm. The drug release behaviour was evaluated up to 03 hr, collecting 5 mL samples at each time point, and determined by UV-spectrophotometry. The readings (in triplicates) were calculated from the calibration curve (Table S3) to obtain the corresponding concentration of the drug across the time profile.³⁷

Stability studies

The formulations were assessed for physical and chemical stability for a period of 06 months in accordance with International Conference on Harmonisation (ICH) guidelines on stability testing of new drug substances and products: ICHQ1A (R2) with accelerated testing at $40^\circ\text{C} \pm 2^\circ\text{C}/75\% \text{RH} \pm 5\% \text{RH}$ up to 6 months.³⁸ They were stored in sealed aluminium packets and the physical characteristics, *in vitro* drug content was determined periodically after 1, 2, 3 and 6 months.

Bioanalytical Method Validation [Ich M10]

To determine the amount of PHL released in the biological matrix (i.e., blood plasma) and gain an improved understanding of PK parameters such as AUC (Area Under the Concentration-time curve) and C_{max} (maximum concentration), the rate and extent of drug absorption was carried out employing a validated HPLC method.

HPLC system and conditions

An RP – HPLC (Jasco LC-4000 series) system with a Photo Diode Array (PDA) UV detector was employed in the study. The stationary phase was a Welchrom C18, 4.6*250 mm, 5 μ pore size column. The mobile phase was a mixture of ACN and MQ water, in a ratio of 40:60 (v/v), and the wavelength (λ_{max}) was set to 286 nm. The solvents were filtered and sonicated before use. Elution

was carried out at a flow rate of 1 mL/min for 10 min (retention time=tR) in isocratic mode. Sample volume injected in the HPLC was 10 μL . Maintaining an ambient temperature of 25°C ensured sharp peaks without any interference. All samples were analysed using the Jasco ChromNAV version 2.03.06 software.

Preparation of Standard and Working Solutions

Initially, a stock solution of 1000 ppm (1 mg/mL) of PHL was prepared in MeOH. It was filtered, if necessary, and remaining dilutions for Working Solutions (WS) were prepared in MeOH. For the calibration study, concentrations ranging from 10-150 ppm were chosen to obtain a standard curve. For method development, an accurate and equivalent amount of blank rat plasma (100 μL) was added to 150 μL of prepared WS and the volume was made up to 500 μL with MeOH. After protein precipitation with MeOH, the mixture was vortexed for 2 min and centrifuged two times at 7000 rpm, 4°C , for 5 min, each. The supernatant was collected in a separate Eppendorf tube and transferred to HPLC vials for further analysis.

Table 1: HPLC parameters for method validation.

Composition	Value
Column	Welchrom C18, 4.6*250 mm, 5 μ pore size
Flow rate (mL/min)	1.0
Retention time (tR)	7.2-7.3
Detector	PDA
Detection wavelength (nm)	286
Injection volume (μL)	10
Temperature ($^\circ\text{C}$)	25
Elution type	Isocratic
Run time (min)	10

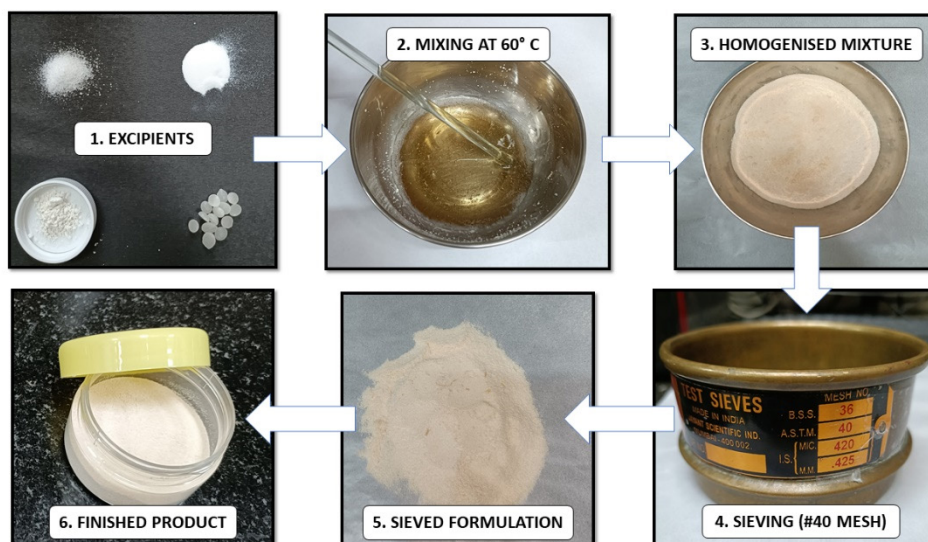


Figure 1: Formulation development by melt-fusion technique.

Sample Preparation

Briefly, in a 1.5 mL Eppendorf tube, 100 μ L of plasma sample (collected at different time points from respective animal groups) was added. To obtain values within the detectable range, a known concentration of standard solution (50 ppm PHL in MeOH) was spiked to all the samples (150 μ L). After vortexing for 1-2 min, 250 μ L MeOH was added to precipitate proteins, volume was made up to 500 μ L, and then vortexed for 1 min. The final mixture was centrifuged for 5 min at 7000 rpm (2 rounds). 10 μ L of the supernatant was collected and analysed according to the same parameters previously validated for the analyte, PHL (Table 1). A slight shift in the tR can be expected owing to the presence of plasma. The corresponding AUCs were subtracted from the AUC value for the spiked sample and the concentration obtained was calculated from the linearity equation ($y=mx+c$).

Pharmacokinetic Analysis

For the PK study, adult SD rats were randomly divided into 04 groups ($n = 06/\text{group}$) viz. GI – IV PHL (10 mg/kg), GII – oral PHL (10 mg/kg), GIII – oral FPOX (10 mg/kg eq.), GIV – oral FGEL (10 mg/kg eq.). PHL and the formulations were suspended in 0.5% sodium Carboxymethyl Cellulose (CMC) and orally administered as a single dose. Blood samples (0.5 mL) were collected at 5, 10, 15, 30, 45 min, 1, 1.5, 2, 4, 6, 8 and 24 hr post-dose with sparse sampling.³⁹ To collect plasma, samples were immediately centrifuged at 2500 rpm for 15 min at 4°C and stored at -80°C until further preparation for HPLC analysis. PK parameters for Non-Compartmental Analysis (NCA) were calculated by the Phoenix[®] WinNonlin[®] (Certara Inc., USA)

software for individual animals and reported as the Mean \pm SD of the group.

Method Validation [adapted from ICH Q2(R1)⁴⁰]

Specificity, Linearity, and Range

The linearity of a method is the ability to maintain a direct proportionality of the results with the concentration of the analyte, within a specific range. Linearity of the plasma samples was calculated from the regression coefficient (R^2) of the graph. 07 aliquots ranging from 10-150 ppm were prepared in MeOH and scanned at λ_{max} of PHL (286 nm) in HPLC. The interval between the highest and the lowest concentrations for which the analytical method gives a sufficient degree of accuracy, precision, and linearity, is termed as range. The same was ascertained from the calibration graph. The specificity of the method was reported to highlight no concomitant interaction of other substances in HPLC.

Accuracy, Precision, and Recovery

To determine the closeness of the readings of the analytical samples and its method to the true or actual values of the standard, can be expressed in its accuracy. This can also be termed as trueness. The mean percentage (%) recovery was calculated as a parameter for accuracy. While, precision is termed as a series of measurements, expressing repeatability and reproducibility, that are obtained over multiple time points from the same homogenous sample. For intra- and inter-day precision, three different concentrations – low, medium, high (30, 70, and 130 ppm) on the same day and once a day for 03 consecutive days, were analysed. The acceptance

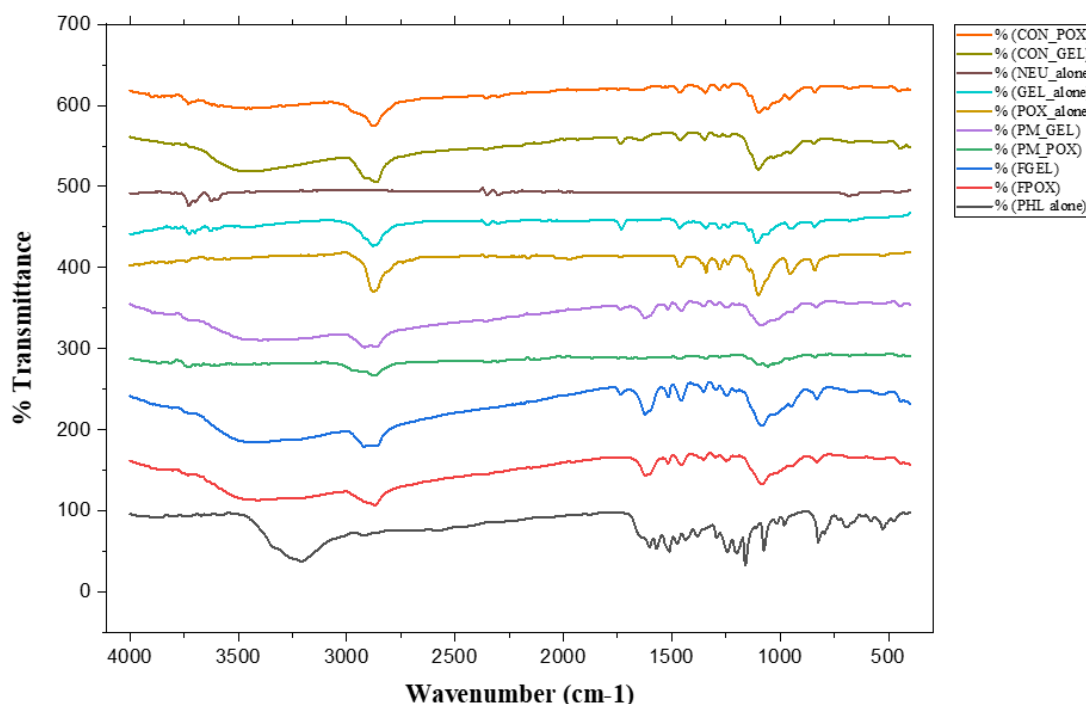


Figure 2: FTIR spectra of different formulations.

criterion was within $\pm 15\%$ deviation from the nominal i.e., Relative SD (RSD).^{41,42}

Robustness

To study how unchanged or resilient the developed method is by making small, but deliberate changes in the method parameters provides an indication of its robustness. 03 different variables were altered; temperature was varied by 3 degrees i.e., 28°C, the wavelength was adjusted by 1, i.e., 285 nm, and the flow rate was adjusted by 1, i.e., 1.1 mL/min keeping the other parameters constant. The %RSD values from the AUC values were calculated and reported.

LOD and LOQ

The lowest amount (concentration) of analyte in a sample which can be detected is termed as the Limit of Detection (LOD) whereas the lowest amount that can be quantified with suitable precision and accuracy is termed as the Limit of Quantification (LOQ) of the developed analytical method. These values can be calculated as follows:

$$\text{LOD} = 3.3 * \sigma / \text{Slope}$$

$$\text{LOQ} = 10 * \sigma / \text{Slope}$$

wherein, σ (sigma) is the Standard Deviation (SD) of the Y-intercept, and S is the mean slope of the calibration curve. It gives an indication of the signal-to-noise ratio.

In vitro Assays

Antioxidant activity

To measure the antioxidant capacity of PHL and the developed formulations, two *in vitro* assays, viz. 1,1-diphenyl-2-picrylhydrazyl (DPPH•) and Oxygen Radical Absorbance Capacity (ORAC) assay were performed.

DPPH• Assay

The DPPH• assay procedure was adapted from Dudonne *et al.*, (2009), to assess the free radical scavenging ability of the flavonoid.⁴³ Briefly, serial dilutions of PHL and its formulations, were prepared alongside ascorbic acid (standard). The solutions were readily mixed with MeOH and 200 μM DPPH was added to the reaction mixture under dark conditions. This 1:1 mixture was incubated at RT for 20 min and absorbance was taken at 517 nm⁴⁴ in a microplate spectrophotometer reader (BioTek Epoch), analysed using Gen5 software. The formula used to calculate the percentage of DPPH•-scavenging activity was

$$\% \text{ DPPH inhibition} = \frac{[\text{Abs}(\text{control}) - \text{Abs}(\text{sample})]}{[\text{Abs}(\text{control})]} * 100$$

ORAC Assay

A prominent technique to measure the scavenging capacity against peroxy Radicals (ROO•) generated by 2,2'-azobis(2-amidinopropane) dihydrochloride (AAPH) using fluorescein as a fluorescence probe is the ORAC assay. AAPH undergoes time-dependent thermal decomposition to form ROO• that quench the fluorescence of fluorescein molecules in

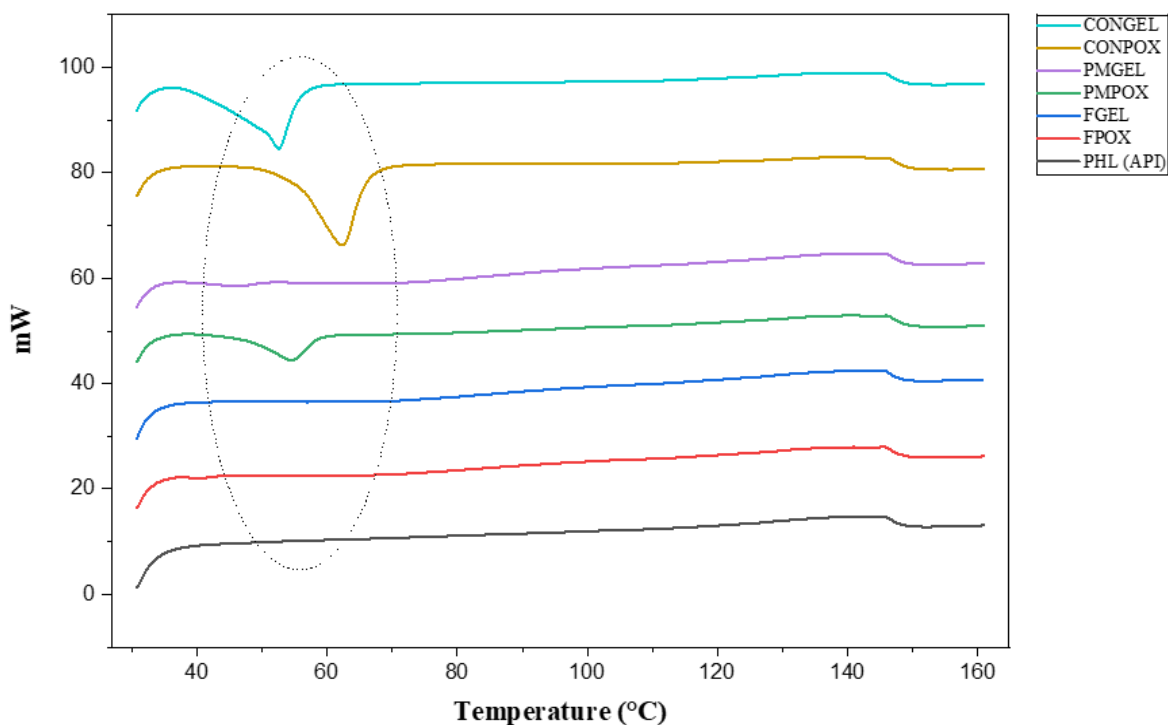


Figure 3: DSC thermal spectra of different formulations.

the reaction mixture. Trolox, a water-soluble vitamin E analogue, is used as the standard. The quenching capacity is measured by calculating the AUC in Trolox equivalents/gram of the formulations. The excitation and emission wavelengths were set at 485 nm and 528 nm, respectively, using a microplate reader. The readings in triplicates were taken across a concentration range and Mean \pm SD of the AUCs were calculated in μ moles of Trolox/gram of sample. The procedure was as described in Deshpande *et al.*, (2023).⁴⁵

Anti-inflammatory Activity – Protein Denaturation Assay

Although carrageenan-induced inflammation is a known technique for measuring the anti-inflammatory potential of drug substances, we employed a simple *in vitro* protein denaturation assay to measure the inhibition in inflammation. The procedure was adapted from earlier reports with modifications.^{46–48} Aspirin, a known Non-Steroidal Anti-Inflammatory Drug (NSAID), was used as a standard. Briefly, 1% bovine serum albumin (BSA, 500 μ L) was added to 100 μ L of sample, and after heating (to enable denaturation), followed by cooling, the absorbance was measured at 660 nm using a microplate reader. Readings were taken in triplicates and % inhibition was plotted for the formulations.

$$\% \text{ inhibition} = 100 - \left\{ \frac{[\text{Abs}(\text{sample}) - \text{Abs}(\text{control})]}{[\text{Abs}(\text{positive control})]} \right\} * 100$$

Statistical Analysis

All the data was represented as Mean \pm SD. The results were analyzed by GraphPad[®] Prism software Ver. 8.0.1 (GraphPad Software, Inc., La Jolla, CA) and performed by OriginPro[®] graphing and analysis software 2025b (OriginLab Corp., Northampton, USA). Statistical significance was considered as $p < 0.05$ in all cases. Wherever necessary, sample sets were analyzed by Student's *t* test for unpaired samples, one-way ANOVA and *post hoc* multiple comparisons tests.

RESULTS AND DISCUSSION

In silico Findings

According to CTD – [chemical-phenotype interaction] query, **91 phenotypes** were found to be associated with PHL [chemical] across Homo sapiens, Mus musculus and Rattus norvegicus [species]. Among those, PHL was found to have a strong involvement in cellular metabolic processes, cell proliferation, cell cycle phases, predominantly mitotic cell cycle processes and S phase, lipid oxidation and catabolism, glutathione transferase activity, ROS biosynthetic process, apoptotic process and glucose import into the cells, lactate dehydrogenase activity, SOD activity and also sperm motility.³⁴ As per reports, PHL has multi-dimensional effects; as a therapy for skin disorders due to enhanced penetration, inhibiting prostaglandins acting as an anti-inflammatory agent, management of diabetes by regulating glucose transport, and inhibiting the pro-inflammatory mediators in macrophages and dendritic cells.^{16,49–51}

Based on the ADMETLab 2.0 simulations data, **88 parameters** were reported. Briefly, PHL satisfied the Lipinski rule of 5,⁵² with a 0.058 probability of P-gp inhibition and very poor BA (<20%) as was indicated by the prominent plasma protein binding (93.96%), and small fraction of drug unbound in plasma (5.864%). It displayed poor BBB penetration (0.023), limited volume of distribution ($V_d = 0.563$), and high rate of clearance ($CL = 15.737$ mL/min/kg) concurring with reports that PHL gets metabolized by conjugative enzymes such as β -glucosidase,¹³ moves rapidly in the intestine, and is efficiently eliminated in the urine.^{53,54} Its drug-likeness score was 0.64 (unattractive), and solubility in water nearly 0.2 mM. These challenges hinder the nutritional and cosmetic applications⁵⁵ of PHL promoting the need to enhance its BA.

Formulation, Development, And Optimisation

In the SE method, a white pasty mixture was obtained and hence could not be evaluated. In the CP method, 30% of P188 enabled the dissemination of PHL uniformly and the solution

Table 2: Formulation development of different batches.

Sr no.	Formulation	Method Ratio	PHL	G48/16	P188	LAB	NEU
			1	3		0.5	2
1	FGEL	Melt-fusion	100 mg	300 mg	-	50 mg	200 mg
2	FPOX	Melt-fusion	100 mg	-	300 mg	50 mg	200 mg
3	PM_GEL	Physical mixture	100 mg	300 mg	-	50 mg	200 mg
4	PM_POX	Physical mixture	-	-	300 mg	50 mg	200 mg
5	CONT_GEL	Only excipient mixture	-	300 mg	-	50 mg	200 mg
6	CONT_POX	Only excipient mixture	-	-	300 mg	50 mg	200 mg

FGEL = formulation with Gelucire 48/16; FPOX = formulation with Poloxamer 188; PM_GEL = physical mixture with Gelucire 48/16; PM_POX = physical mixture with Poloxamer 188; CONT_GEL = physical mixture with Gelucire 48/16 (without API); CONT_POX = physical mixture with Poloxamer 188 (without API).

remained stable up to 48 hr with no crystal formation. P188 showcases reverse solubility at low temperatures due to the hydration capacity of the block copolymer that accelerates drug dissolution.⁵⁶ This technique could be advantageous for developing *in situ* gels.⁵⁷ However, for our study, we chose to proceed with MF method due to its ease and reproducibility. A

step-down approach was employed. Several ratios were attempted for drug loading capacity. Finally, a ratio of 1:3 of drug: polymer was selected due to the effectiveness and stability of P188. PHL got completely embedded within the polymer (P188) producing a white crystalline homogenous mixture. This can be attributed to the low melting point and increased wettability of P188.⁵⁸ Based

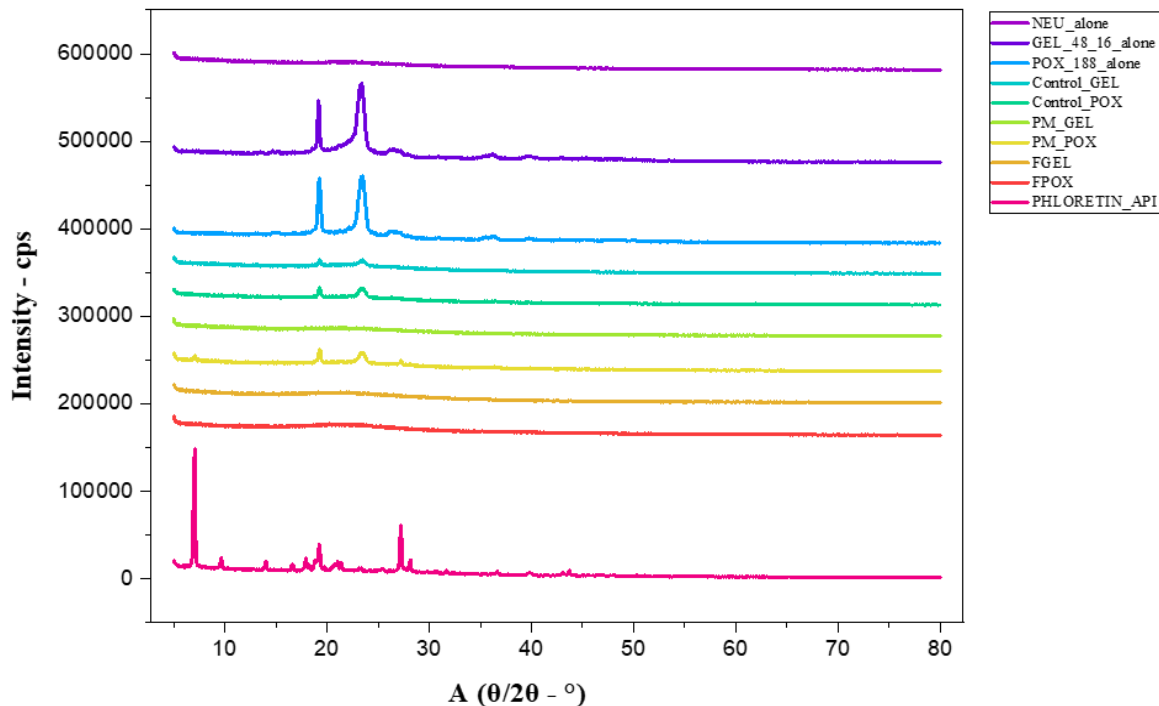
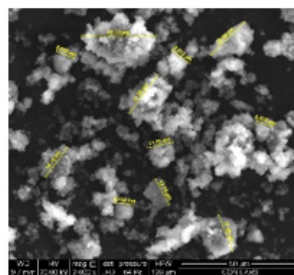
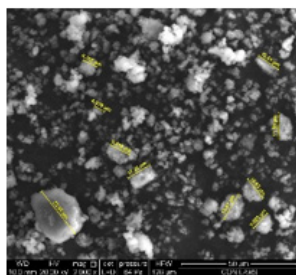
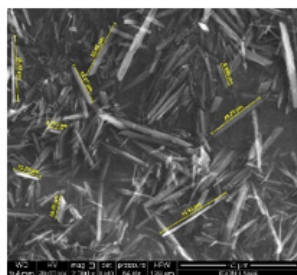


Figure 4: X-ray diffractogram of different formulations.

PHL API

FPOX

FGEL



PM_POX

PM_GEL

CONT_POX

CONT_GEL

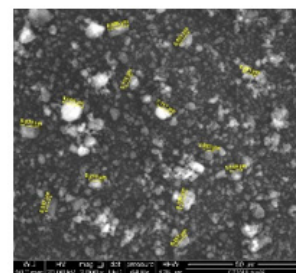
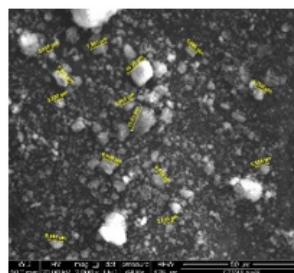
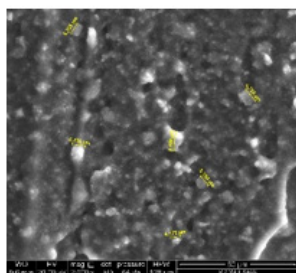
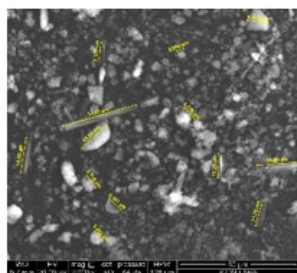


Figure 5: SEM images of different formulations (at 2000x magnification).

on this ratio, the final formulations were prepared as shown in Figure 1, Table 2.

Characterisation

FTIR

A cumulative FTIR spectra of %transmittance vs. wavenumber (cm^{-1}) was obtained for all the formulations (Figure 2). PHL is a dihydrochalcone flavonoid containing multiple alcoholic groups. With respect to the FTIR scan for PHL, the strong and broad O-H stretching at 3208.97 cm^{-1} can also be observed in the formulations FPOX (3414.35 cm^{-1}) and FGEL (3435.56 cm^{-1}). Additional O-H stretching can be observed for both the polymers FPOX 2870.52 cm^{-1} and FGEL 2917.77 cm^{-1} depicting its unique presence in the formulation. PHL possesses phenyl rings (cyclic alkene). This C=C stretching ($1566\text{-}1650 \text{ cm}^{-1}$) is observed at 1603.52 cm^{-1} in PHL, at 1621.84 cm^{-1} in FPOX and 1623.77 cm^{-1} in FGEL. The presence of 2 phenyl rings gives an indication of secondary alcoholic groups that are depicted at 1075.12 cm^{-1} , 1083.8 cm^{-1} , and 1082.83 cm^{-1} and the peak of C-H stretching in methyl groups is at 1475.28 cm^{-1} , 1455.03 cm^{-1} , and 1456.96 cm^{-1} for PHL, FPOX, and FGEL, respectively. The variations in the intensities and shapes of the peaks can be attributed to physical interactions between PHL and the polymers.

DSC

For both the polymers GEL and P188, the melting point (T_m ; $q=6\text{-}7 \text{ mW}$) was $\sim 60^\circ\text{C}$, this endothermic reaction was seen by a dip in the graph (Figure 3). The glass transition temperature (T_g) was between $150\text{-}160^\circ\text{C}$. The processing temperature for the technique should hence lie between $60\text{-}160^\circ\text{C}$ ($>T_m$ and $<T_g$). Phase change was observed above 160°C suggesting polymerisation of the polymers. For both the formulations, FGEL and FPOX the dip was not observed suggesting that PHL was embedded in the polymer matrix owing to a partial amorphization of the crystalline structure. Therefore, hot melt-fusion is essential for completing the reaction. Conversely, in the physical mixture of PHL, i.e., PM_POX, a dip was observed suggesting that the homogenous mixing between the drug and excipients had not been carried out. Today, the highest number of drugs ($>50\%$) in the pharmaceutical pipeline belong to BCS class II. Among the strategies for development of ASDs, freeze drying, fluid-bed coating, spray drying, co-precipitation method, and HME technique, are popular.⁵⁹ The ASDs prevented recrystallisation or degradation of the API even at higher temperatures, offering stability.⁶⁰

XRD

The XRD plot for PHL revealed the characteristic peaks corresponding to the native crystalline structure of PHL at 7.005° ,

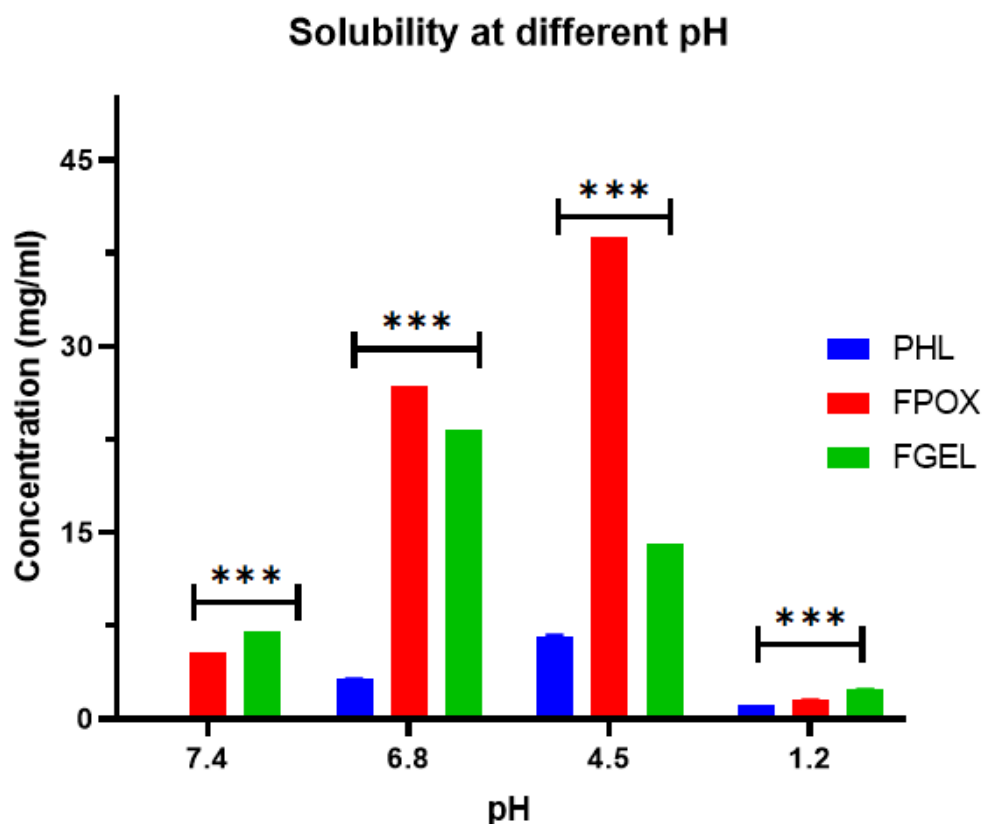


Figure 6: Concentration (mg/mL) of formulations soluble at different pH.

9.638°, 14.007°, 19.236°, and 27.209°. From Figure 4, peaks for FPOX and FGEL, it was evident that the crystalline nature of PHL got completely masked due to its incorporation in the polymer matrix as no clear strong peak was observed. PHL was uniformly distributed in the formulation making it amorphous.⁶¹ The intensity was measured against $2\theta^\circ$ values. Both DSC and XRD data confirmed the formation of ASDs of PHL, known as FPOX and FGEL, in the polymeric blends of P188 and GEL48/16, respectively, with NEU and LAB as excipients.

SEM

As observed in Figure 5, PHL retained its crystalline structure, whereas the formulations, FPOX and FGEL, completely entrapped the drug into their polymer matrix (all images were taken at 100 μm , 1000X magnification). Interestingly, the physical mixtures, i.e., PM_POX and PM_GEL did not completely integrate the drug into the mix highlighting the need for melt-fusion technology. When observed at 50 μm , the particle size of PHL was found to be in the range of 10.35 – 33.83 μm , FPOX – 4.978 – 23.58 μm , and FGEL – 8.078 – 21.0 μm .

In vitro Release

Saturation Solubility, Dissolution, and Stability

The percent drug release at pH 1.2 of PHL alone was closely matched with FPOX whereas FGEL was significantly poor ($p < 0.001$, Figure 6) in its release over time suggesting that it was unstable for a longer duration. The poor solubility of PHL in water (pH 7.4) limits its therapeutic potential⁶²⁻⁶⁴ highlighting the need for ASDs. FPOX would be an improved and preferred formulation as was noted in its significantly enhanced solubility at pH=1.2, 4.5, 6.8, and 7.4 (Figure 7). Li *et al.*, (2011) described the

solubility of PHL in different solvents according to the theory of solid-liquid phase equilibrium. They suggested that the solubility of PHL is directly proportional to temperature, with MeOH and ethanol showing dominant solubility over other solvents.⁵⁴ Estimating for stability over 6 months, % drug content for FPOX and PM_POX was equivalent to that of PHL API (Figure 8) in the range of 90-110%. Surprisingly, the increase in % drug content for FGEL and PM_GEL can be attributed to elution of the drug from the formulation, interaction with the components of the mixture, degradation of the active ingredient, or formation of an unintended by-product. Initially, the formulations, FGEL and PM-GEL were cream-white free-flowing powders, but they obtain a semi-solid orange gel-like consistency upon long-term storage suggesting instability. PHL and FPOX, however, remain unchanged (white fluffy powder and cream-white powder).

Bioanalytical Method Validation

Pharmacokinetic Analysis

The results of the PK analysis were on the assumption that the biological system is a single unit i.e., NCA. The release followed first-order kinetics, i.e., a direct co-relationship between the amount of drug released in the body (concentration in $\mu\text{g/mL}$) with respect to time (hr). The trapezoidal rule was utilized to calculate the extent of drug exposure employing the Phoenix' software. Since IV PHL has the maximum exposure being administered directly into the systemic circulation (100% BA), the initial concentration i.e., C_0 was 8820.68 ± 6623.48 ng/mL. Other prominent features, viz. C_{max} , T_{max} (time to maximum concentration), AUC, and %F (percent BA) were recorded in Table 3. C_{max} for IV PHL was >2-fold than the oral PHL group (33.96 ± 2.60 $\mu\text{g/mL}$ vs. 17.83 ± 5.12 $\mu\text{g/mL}$ respectively), whereas

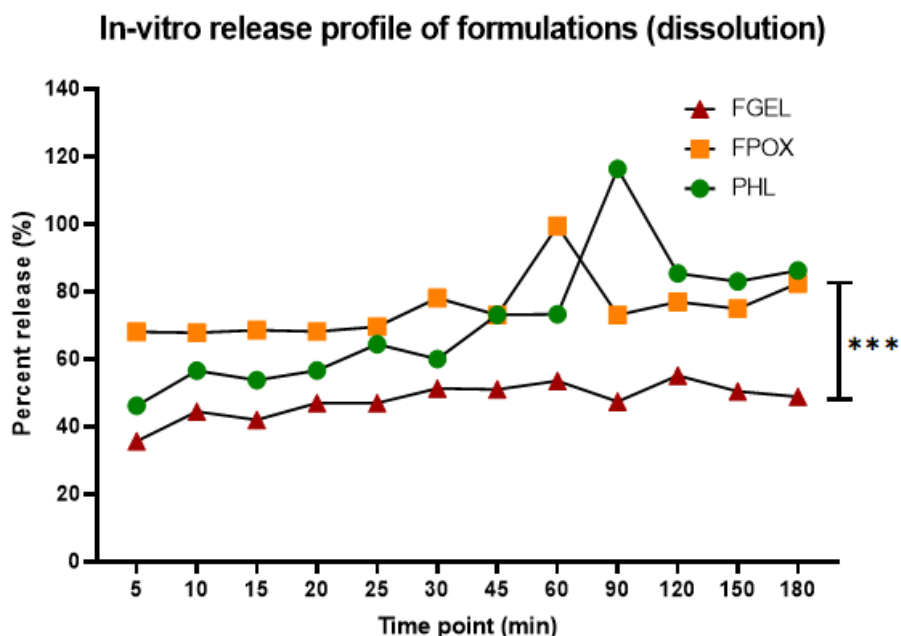


Figure 7: Percent release of formulations vs. time (min).

the oral formulation groups (FPOX and FGEL), although not significant, showed a marginal improvement over the API (FPOX: $21.41 \pm 2.65 \mu\text{g/mL}$; FGEL: $20.42 \pm 2.21 \mu\text{g/mL}$). Interestingly, we found that the AUC (last) values for both the formulations were nearly 3-fold higher compared to the API (oral PHL: $14.98 \pm 4.91 \text{ hr} \cdot \mu\text{g/mL}$ vs. FPOX: $54.60 \pm 30.0 \text{ hr} \cdot \mu\text{g/mL}$ and FGEL: $67.76 \pm 23.83 \text{ hr} \cdot \mu\text{g/mL}$). T_{max} was attained quickly not only for IV ($0.20 \pm 0.05 \text{ hr}$) but also oral PHL (API = 0.167 hr), while the oral formulations took longer (FPOX: $5 \pm 3.5 \text{ hr}$ and FGEL: $0.7 \pm 0.1 \text{ hr}$) to achieve the highest concentration in the body. The MRTlast (h), i.e., suggestive of the average time that all the molecules of a formulation spend in the body, were superior for both the formulations, (FPOX and FGEL) vs. oral API (3.8375 ± 1.231 and 4.012 ± 1.806 vs. 3.249 ± 1.453 respectively).

From Figure 9A, it is evident that PHL (API) had very poor BA and release over time, whereas FPOX showed a significant improvement over PHL (%F = 37.96 vs. 10.42 ; $p < 0.01$). FGEL although at par with FPOX, was not preferred due to its instability (Figure 9B). Lastly, reports suggest that masking the phenolic -OH groups by acetylation could increase the BA and duration of action of PHL,⁶⁵ however, its penetration into the brain was unchanged. Our results showed that the concentration of PHL in the brain, when administered systemically, was $49.21 \pm 4.40 \mu\text{g/mL}$ whereas FPOX had a superior brain distribution compared to its API ($78.69 \pm 9.02 \mu\text{g/mL}$ vs. $64.33 \pm 6.45 \mu\text{g/mL}$ respectively, $*p < 0.05$).

Method Validation

Specificity, Linearity, and Range

The developed method was highly specific; no other peak was obtained while running the samples. Figure 10A shows the calibration curve over the range $10 - 150 \mu\text{g/mL}$ suggesting a linear relationship of AUC values plotted against the concentration ($n=3$). The straight-line equation obtained was $y = 10272x - 43205$ and regression coefficient $R^2 = 0.9915$. Figure 10B depicts the linearity overlay of the working standard solutions in HPLC.

Accuracy, Precision, and Recovery

To study system suitability, 06 replicates of the same concentration (50 ppm) were run in HPLC (Table 4.1). To estimate accuracy and recovery, the average readings of the spiked samples were calculated against the obtained values and % recovery was noted in the Table 4.2. For precision, intra-day and inter-day, 03 concentrations were run in triplicates³⁹ and readings obtained demonstrated appreciable reproducibility of the method (Table 4.3). All data were expressed in mean AUC values with %RSD $< 15\%$.

Robustness

Based on the 03 parameters that were altered (temperature, flow rate, wavelength), the results of robustness were depicted in the Table 4.4. As per the bioanalytical guidelines, the %RSD was less than 10% across all 03 concentration levels. The ideal HPLC conditions were as follows: Temperature - 25°C , Flow Rate (FR) - 1 mL/min , Wavelength (WL) - 286 nm ($n=3$ at each level).

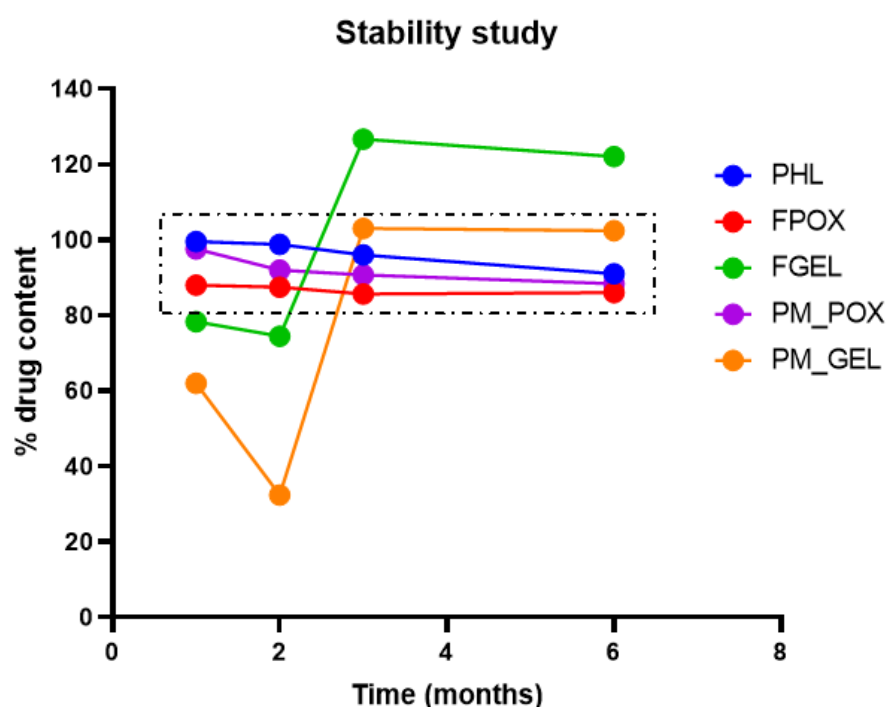
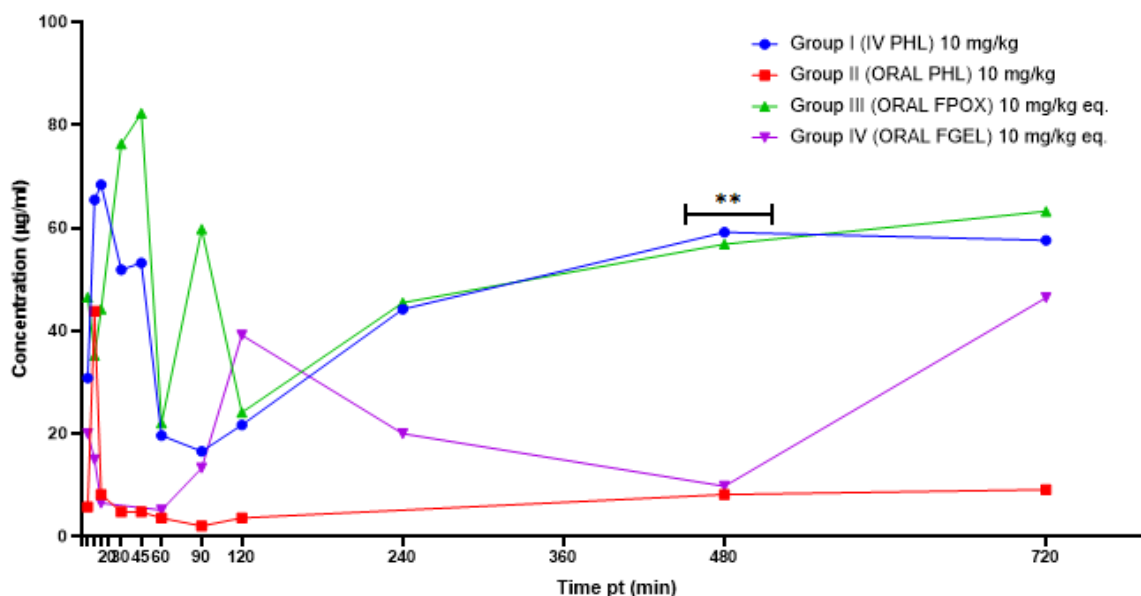


Figure 8: Stability study of different formulations.

Table 3: Pharmacokinetic profile of different formulations.

Parameters	IV PHL API	Oral PHL API	Oral PHL formulation (FGEL)	Oral PHL formulation (FPOX)
Dose (mg/kg)	10	10	10 eq.	10 eq.
C _{max} (ng/mL)	33960.005±2607.354	17832.09±5123.109	21416.515±2649.551	20422.3625±2207.841
T _{max} (h)	0.209±0.048	0.167	5±3.464	0.6875±0.125
AUC (last) (h*ng/mL)	143833.313±56223.432	14981.693±4908.232	54605.514±29968.606	67766.5425±23828.35
AUCINF_obs (h*ng/mL)	232595.618	20328.355±9060.65	-	-
MRT _{last} (h)	3.976±1.251	3.249±1.453	4.012±1.806	3.8375±1.231
MRTINF (h)	9.4	6.871±5.071	-	-
CL_obs (mL/h/kg)	42.993	-	-	-
V _{ss_obs} (mL/kg)	404.131	-	-	-
F% (bioavailability)	-	10.42	47.11	37.96

C_{max} = maximum (peak) concentration; T_{max} = time to maximum (peak) concentration; AUC = Area Under Curve; MRT = Mean Residence Time; CL_obs = clearance; V_{ss_obs} = volume of distribution at steady-state.

Pharmacokinetic profile (in-vivo drug release)**Figure 9A:** Pharmacokinetic profile (concentration vs. time) for different animal groups.

LOD and LOQ

For reporting, the S (mean of slope) = 10272.21, and σ (SD) = 535094.8 were calculated from the calibration graph, the LOD and LOQ for PHL was found to be 12.41 $\mu\text{g/mL}$ and 37.61 $\mu\text{g/mL}$ respectively, i.e., LOQ was nearly 3-fold of LOD. The specificity of the method was thus established as the lowest concentration in linearity (10 $\mu\text{g/mL}$) was very close to the LOD value.

In vitro Assays

Antioxidant Assays (DPPH● and ORAC)

In the DPPH assay (Figure 11), the IC₅₀ ($\mu\text{g/mL}$) values of ascorbic acid (standard) were presumably lowest at 4.66 $\mu\text{g/mL}$. The values for PHL (API) were closely matched with its formulations FPOX and PM_POX (80.43 $\mu\text{g/mL}$ vs. 87.98 $\mu\text{g/mL}$; 90.44 $\mu\text{g/mL}$

$\mu\text{g/mL}$ respectively; $p < 0.05$). The formulations FGEL, and PM_GEL however, were not significant (100.75 $\mu\text{g/mL}$ and 229.31 $\mu\text{g/mL}$, respectively). These results confirm that the antioxidant capacity of PHL was retained in the formulations. DPPH assay can hence be used as a preliminary tool to measure the ROS-scavenging potential of a drug.⁶⁶

For the ORAC score, the calibration graph for equating Trolox equivalents was calculated. As shown in Figure 12, the Mean \pm SD of the AUCs were calculated in μmoles of Trolox/gram of sample observed in lakhs. The ORAC score for PHL was 122.70 lakhs, whereas the formulation FPOX showed >2-fold improvement in the score (277 lakhs; $p < 0.0001$) and FGEL as well at 219 lakhs ($p < 0.01$). Further, the physical mixtures, PM_POX and PM_GEL also demonstrated notable free radical-scavenging capacities

Table 4: Bioanalytical validation parameters for HPLC**Table 4.1: Bioanalytical validation parameters for HPLC – System suitability**

Concentration (ppm)	Parameter			
50	AUC		tR	
	Mean	%RSD	Mean	%RSD
	408130.8	7.90	7.290	2.04

Table 4.2: Bioanalytical validation parameters for HPLC - Accuracy

Concentration (ppm)	Mean recovery (ppm)	%Recovery	%RSD
50	53.36	106.73	13.24
100	99.97	99.97	2.20
150	156.43	104.29	11.44

Table 4.3: Bioanalytical validation parameters for HPLC – Precision

Parameters	Concentration (ppm)	Mean AUC±SD	%RSD
INTRA-DAY	30	282744.3±9069.91	3.207813
Repeatability	70	596875.7±12052.21	2.019215
	130	1234635±20870.24	1.690398
Parameters	Concentration (ppm)	Mean AUC±SD	%RSD
INTER-DAY	30	304939.7±32946.14	10.80415
Intermediate	70	614730.7±26700.22	4.343402
	130	1227362±31812.57	2.591948

Table 4.4: Bioanalytical validation parameters for HPLC - Robustness

Parameters	Concentration (ppm)	Mean AUC±SD	%RSD	Mean tR±SD	tR %RSD
Temperature (28 °C)	30	254411.3±24557.00	9.652	7.35±0.190	2.591
(Temperature = 28 °C, FR=1, WL=286 nm)	70	569676±21122.96	3.707	7.31±0.179	2.449
	130	1211031±23971.48	1.979	7.35±0.140	1.908
Flow rate (1.1 ml/min)	30	254718.3±24112.52	9.466	7.17±0.447	6.234
(Temperature = 25 °C, FR=1.1, WL=286 nm)	70	562721±32298.13	5.740	7.17±0.387	5.397
	130	1180551±75971.21	6.435	7.17±0.394	5.491
Wavelength (285 nm)	30	263353±14303.72	5.431	7.42±0.160	2.149
(Temperature = 25 °C, FR=1, WL=285 nm)	70	581610.7±9903.595	1.702	7.40±0.123	1.666
	130	1220872±9331.789	0.764	7.39±0.134	1.816

Plasma concentration vs. time

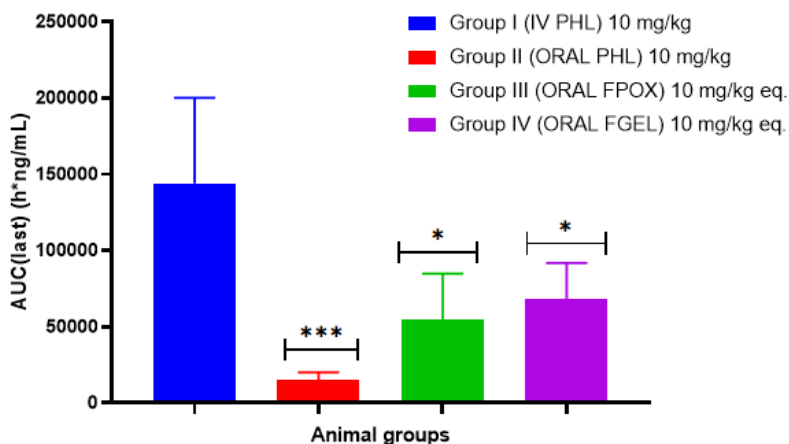


Figure 9B: Pharmacokinetic profile (AUClast) (h*ng/mL) for different animal groups.

Linearity of PHL in plasma

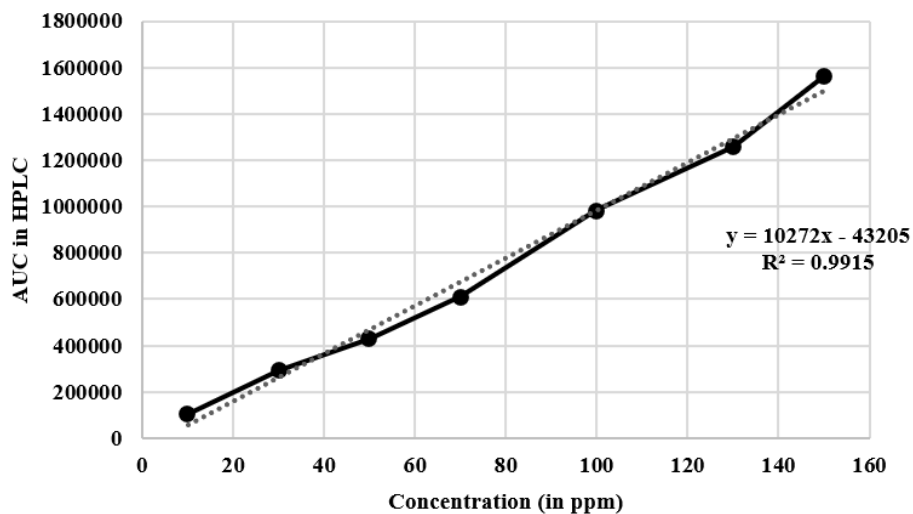


Figure 10A: Calibration curve for PHL in plasma using RP-HPLC.

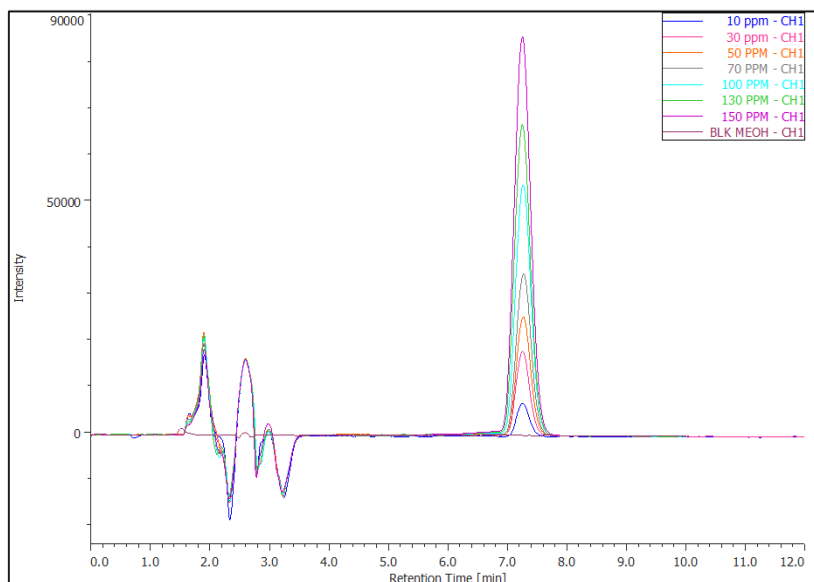


Figure 10B: Linearity overlay of PHL in plasma using RP-HPLC.

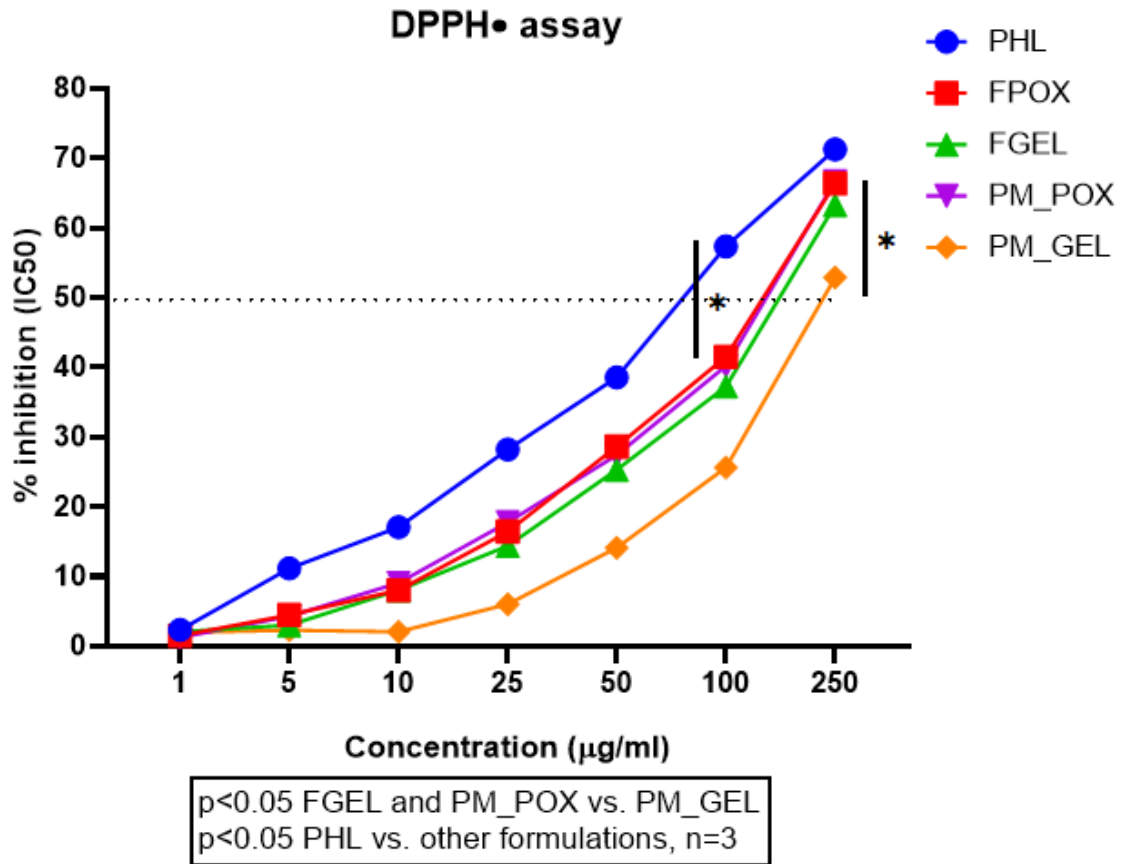


Figure 11: DPPH assay measuring anti-oxidant activity.

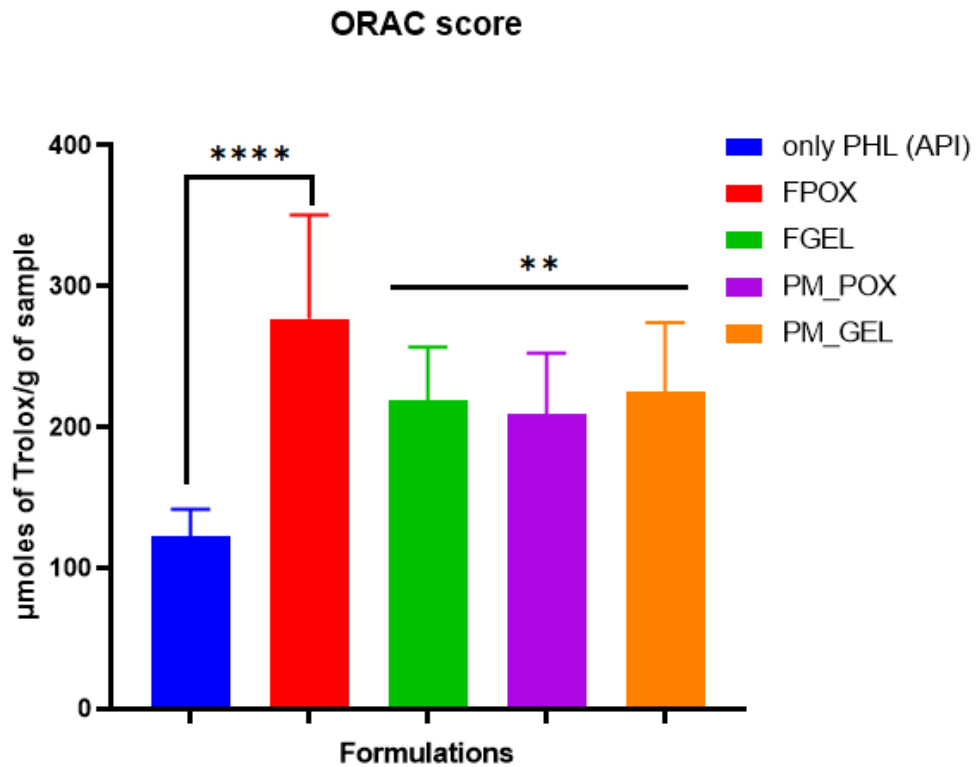


Figure 12: ORAC assay measuring anti-oxidant activity.

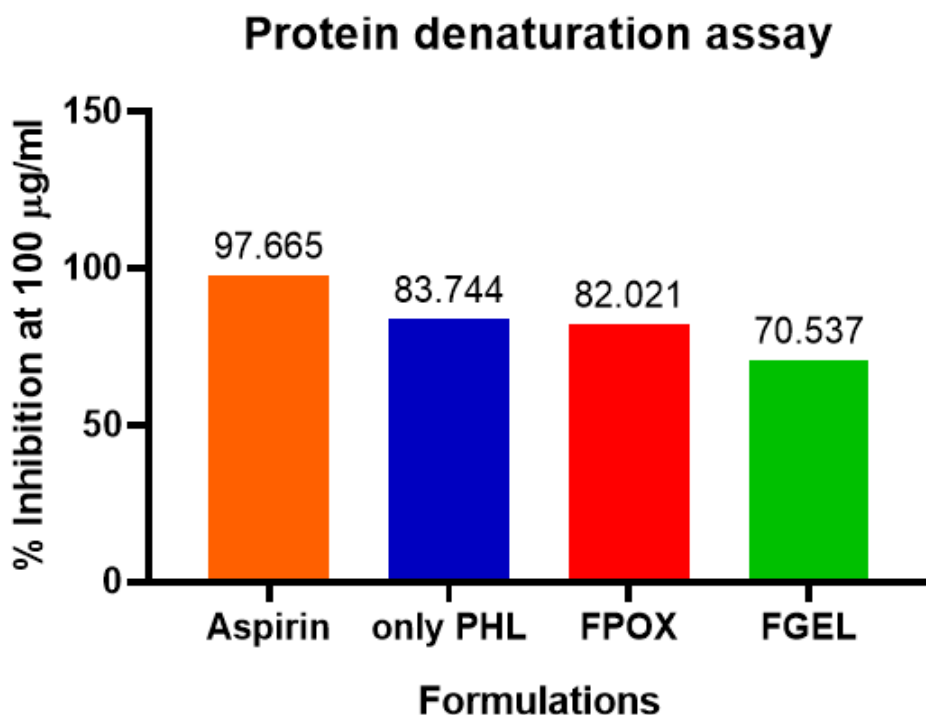


Figure 13: Anti-inflammatory assay (protein inhibition).

(209.50 lakhs; $p < 0.01$; 224.56 lakhs; $p < 0.01$) highlighting the pronounced antioxidant activity of PHL. The ORAC score is thus a reliable parameter, and more definitive as it employs a biological standard.^{67,68} Among several reports, it is evident that the stronger antioxidant potential of PHL is due to its multiple -OH groups.⁶⁹ Moreover, the number, relative position of -OH groups, and presence of an alkyl chain make it distinctly effective than other dihydrochalcones.⁷⁰ In antioxidant assays like FRAP, ABTS, and DPPH●, PHL has much lower IC_{50} values compared to its glycosylated congeners (phloridzin, trilobatin, naringin dihydrochalcone, and neohesperidin dihydrochalcone) asserting that the glycosylation of -OH reduces its antioxidant capacity, especially electron transfer, hydrogen atom transfer and formation of radical adducts.⁷¹ As was also observed for flavonoids like dihydromyricetin,⁷² baicalein, and baicalin.⁷³

Anti-inflammatory Assay – Protein Denaturation

In the protein denaturation assay (Figure 13), to measure the percentage inhibition, both FPOX and PHL, at 100 µg/mL, had equivalent values (83.74% and 82.02% respectively) whereas FGEL was marginally lower (70.54%) when compared with the standard NSAID, aspirin (98% with $IC_{50} \sim 20$ µg/mL). A host of literature suggests that PHL exerts anti-inflammatory protection. Several autoimmune disorders that identify with inflammation as a core component, might be benefited from PHL and its formulations. PHL inhibits NF- κ B/MAPK and GLUT1-driven

cytokine release, enhances Nrf2/HO-1 antioxidant defence, and suppresses immune cell and tissue injury (inhibits the release of PGE2 and suppresses COX-2 expression) across various models.^{74,75} The anti-inflammatory property of PHL was thus retained as the formulations demonstrated prominent results.

CONCLUSION

We utilised a three-pronged approach in our study. First, utilising different polymers and techniques, a bio-enhanced oral formulation of PHL i.e., FPOX was developed and characterised using sophisticated tools, to demonstrate increased drug-permeation, solubility, and stability, as compared to FGEL and the corresponding API. Second, its BA *in vivo* and brain distribution, was established using a validated bioanalytical HPLC method. Third, the pronounced antioxidant and anti-inflammatory potential of PHL was boosted in its ASD i.e., FPOX through *in vitro* assays. Further studies can be carried out to explore the neuroprotective role of FPOX in behavioural animal models, establishing its significance as a potent therapeutic agent in conditions like AD.

ACKNOWLEDGEMENT

The authors acknowledge A. Kharat, M. Kshirsagar, S. Gurram, for their timely inputs, and the Department of Pharmaceutical Sciences and Technology, Institute of Chemical Technology, Mumbai, India for infrastructural support.

ABBREVIATIONS

API: Active Pharmaceutical Ingredient; **CMC:** Sodium Carboxymethyl Cellulose; **ASD:** Amorphous Solid Dispersion; **SD:** Solid Dispersion; **DSC:** Differential Scanning Calorimetry; **XRD:** X-ray Diffraction; **FTIR:** Fourier-Transform Infrared Spectroscopy; **SEM:** Scanning Electron Microscopy; **RP-HPLC:** Reverse Phase-High Performance Liquid Chromatography; **PDA:** Photo Diode Array; **PK:** Pharmacokinetic profiling; **BBB:** Blood-Brain Barrier; **BCS:** Biopharmaceutics Classification System; **AUC:** Area Under the Concentration-time curve; **C_{max}**: Maximum concentration attained in the body; **T_{max}**: Time to maximum concentration.

FUNDING SOURCES

This research did not receive any specific grant from funding agencies in the public, commercial, or not-for-profit sectors.

CONFLICT OF INTEREST

The authors declare that there is no conflict of interest.

REFERENCES

- Grabska-Kobyłecka I, Szpakowski P, Król A, Książek-Winiarek D, Kobyłecki A, Głabiński A, *et al.* Polyphenols and Their Impact on the Prevention of Neurodegenerative Diseases and Development. *Nutrients*. 2023;15(15).
- Yan L, Guo MS, Zhang Y, Yu L, Wu JM, Tang Y, *et al.* Dietary plant polyphenols as the potential drugs in neurodegenerative diseases: current evidence, advances, and opportunities. *Oxid Med Cell Longev*. 2022.
- Williamson G, Kay CD, Crozier A. The Bioavailability, Transport, and Bioactivity of Dietary Flavonoids: A Review from a Historical Perspective. *Compr Rev Food Sci Food Saf* [Internet]. 2018; 2022: 1054-112. doi: 10.1155/2022/5288698, PMID 35237381.
- Gonzalez-Alfonso JL, Alonso C, Poveda A, Ubiparip Z, Ballesteros AO, Desmet T, *et al.* Strategy for the enzymatic acylation of the apple flavonoid phloretin based on Prior α -glucosylation. *J Agric Food Chem*. 2024; 72(8): 4325-33. doi: 10.1021/acs.jafc.3c09261, PMID 38350922.
- Andrés Juan C, Manuel Pérez de la Lastra J, Plou FJ, Pérez-Lebeña E, Reinbothe S. Molecular sciences the chemistry of reactive oxygen species (ROS) revisited: outlining their role in biological macromolecules (DNA, lipids and proteins) and induced pathologies. *Int J Mol Sci* [Internet]. 2021;22:4642. doi: 10.3390/ijms.
- Al Mamun AA, Shao C, Geng P, Wang S, Xiao J. Polyphenols targeting NF- κ B pathway in neurological disorders: what we know so far? *Int J Biol Sci* [Internet]. 2024;20(4):1332-55. doi: 10.7150/ijbs.90982, PMID 38385077.
- Arias-Sánchez RA, Torner L, Fenton Navarro B. Polyphenols and neurodegenerative diseases: potential effects and mechanisms of neuroprotection. *Molecules* [Internet]. 2023;28(14):5415. doi: 10.3390/molecules28145415, PMID 37513286.
- Jia Y, Wang Y, Wang Z, Zhang Z, Zhang J, Zhang J, *et al.* Neuroprotective effects of total phenolics from *Hemerocallis citrina* Baroni leaves through the PI3K/AKT pathway. *Front Pharmacol*. 2024;15:1370619. doi: 10.3389/fphar.2024.1370619, PMID 39070797.
- Zhang W, Zhuang S, Guan H, Li F, Zou H, Li D. New insights into the anti-apoptotic mechanism of natural polyphenols in complex with Bax protein. *J Biomol Struct Dyn* [Internet]. 2024;42(6):3081-93. doi: 10.1080/07391102.2023.2212066, PMID 37184126.
- Hyson DA. A comprehensive review of apples and apple components and their relationship to human health. *Adv Nutr*. 201; 2(5):408-20. doi: 10.3945/an.111.000513, PMID 22332082.
- Oyenihi AB, Belay ZA, Mditshwa A, Caleb OJ. 'An apple a day keeps the doctor away': the potentials of apple bioactive constituents for chronic disease prevention. *J Food Sci*. 2022;87(6):2291-309. doi: 10.1111/1750-3841.16155, PMID 35502671.
- Rana S, Bhushan S. Bhushan S. Apple phenolics as nutraceuticals: assessment, analysis and application. *J Food Sci Technol* [Internet]. 2016; 53(4):1727-38. doi: 10.1007/s13197-015-2093-8, PMID 27413201.
- Crespy V, Morand C, Besson C, Manach C, Démigné C, Rémésy C. Comparison of the intestinal absorption of quercetin, phloretin and their glucosides in rats. *J Nutr*. 2001;131(8):2109-14. doi: 10.1093/jn/131.8.2109, PMID 11481403.
- Boyer J, Liu RH. Apple phytochemicals and their health benefits. *Nutr J*. 2004;3(1):5. doi: 10.1186/1475-2891-3-5, PMID 15140261.
- Nakhate KT, Badwaik H, Choudhary R, Sakure K, Agrawal YO, Sharma C, *et al.* Therapeutic potential and pharmaceutical development of a multitargeted flavonoid phloretin. *Nutrients*. 2022;14(17):3638. doi: 10.3390/nu14173638, PMID 36079895.
- Ying Y, Jiang C, Zhang M, Jin J, Ge S, Wang X. Phloretin protects against cardiac damage and remodeling via restoring SIRT1 and anti-inflammatory effects in the streptozotocin-induced diabetic mouse model. *Aging* (Albany, NY) [Internet]. 2019;11(9):2822-35. doi: 10.18632/aging.101954, PMID 31076562.
- Sampath C, Sang S, Ahmedna M. *In vitro* and *in vivo* inhibition of aldose reductase and advanced glycation end products by phloretin, epigallocatechin 3-gallate and [6]-gingerol. *Biomed Pharmacother* [Internet]. 2016;84:502-13. doi: 10.1016/j.biopha.2016.09.073, PMID 27685794.
- Han L, Li J, Li J, Pan C, Xiao Y, Lan X, *et al.* Activation of AMPK/Sirt3 pathway by phloretin reduces mitochondrial ROS in vascular endothelium by increasing the activity of MnSOD via deacetylation. *Food Funct* [Internet]. 2020;11(4):3073-83. doi: 10.1039/C9FO02334H, PMID 32195489.
- Barrea D, Currò M, Bellocchio E, Ficarra S, Laganà G, Tellone E, *et al.* Neuroprotective effects of phloretin and its glycosylated derivative on rotenone-induced toxicity in human SH-SY5Y neuronal-like cells. *BioFactors*. 2017;43(4):549-57. doi: 10.1002/biof.1358, PMID 28401997.
- Ghumatkar PJ, Patil SP, Peshattiar V, Vijaykumar T, Dighe V, Vanage G, *et al.* The modulatory role of phloretin in A β 25-35 induced sporadic Alzheimer's disease in rat model. *Naunyn Schmiedeberg's Arch Pharmacol*. 2019 Mar 5;392(3):327-39. doi: 10.1007/s00210-018-1588-z, PMID 30488341.
- Bondonno NP, Dalgaard F, Kyrø C, Murray K, Bondonno CP, Lewis JR, *et al.* Flavonoid intake is associated with lower mortality in the Danish Diet Cancer and Health Cohort. *Nat Commun* [Internet]. 2019;10(1):1-10. doi: 10.1038/s41467-019-11622-x, PMID 31409784.
- Andrés CM, Pérez de la Lastra JM, Juan CA, Plou FJ, Pérez-Lebeña E. Polyphenols as antioxidant/pro-oxidant compounds and donors of reducing species: relationship with human antioxidant metabolism. *Processes*. 2023;11(9): 2771 [Internet]. doi: 10.3390/pr11092771.
- Mucha P, Skocznyńska A, Malecka M, Hikisz P, Budzisz E. Overview of the antioxidant and anti-inflammatory activities of selected plant compounds and their metal ions complexes. *Molecules*. 2021;26(16):4886 [Internet]. doi: 10.3390/molecules26164886, PMID 34443474.
- Abu-Azzam O, Nasr M. Nasr M. *In vitro* anti-inflammatory potential of phloretin microemulsion as a new formulation for prospective treatment of vaginitis. *Pharm Dev Technol* [Internet]. 2020;25(8):930-5. doi: 10.1080/10837450.2020.1764032, PMID 32363977.
- Vo CL, Park C, Lee BJ. Current trends and future perspectives of solid dispersions containing poorly water-soluble drugs. *Eur J Pharm Biopharm* [Internet]. 2013; 85(3 Pt B):799-813. doi: 10.1016/j.ejpb.2013.09.007, PMID 24056053.
- Wei Y, Zhang J, Memon AH, Liang H. Molecular model and *in vitro* antioxidant activity of a water-soluble and stable phloretin/hydroxypropyl- β -cyclodextrin inclusion complex. *J Mol Liq* [Internet]. 2017;236:68-75. doi: 10.1016/j.molliq.2017.03.098.
- Zhang M, Zhuang X, Li S, Wang Y, Zhang X, Li J, *et al.* Designed fabrication of phloretin-loaded propylene glycol binary ethosomes: stability, skin permeability and antioxidant activity. *Molecules*. 2023;29(1): 66. doi: 10.3390/molecules29010066, PMID 38202649.
- Wang Y, Li D, Lin H, Jiang S, Han L, Hou S, *et al.* Enhanced oral bioavailability and bioefficacy of phloretin using mixed polymeric modified self-nanoemulsions. *Food Sci Nutr*. 2020;8(7):3545-58. doi: 10.1002/fsn3.1637, PMID 32724617.
- Newa M, Bhandari KH, Li DX, Kwon TH, Kim JA, Yoo BK, *et al.* Preparation, characterization and *in vivo* evaluation of ibuprofen binary solid dispersions with Poloxamer 188. *Int J Pharm* [Internet]. 2007;343(1-2):228-37. doi: 10.1016/j.ijpharm.2007.05.031, PMID 17597315.
- Shinde UK, Suryawanshi DG, Amin PD. Development of Gelucire® 48/16 and TPGS mixed micelles and its pellet formulation by extrusion spherulization technique for dissolution rate enhancement of curcumin. *AAPS PharmSciTech*. 2021;22(5):182. doi: 10.1208/s12249-021-02032-8, PMID 34129146.
- Xie B, Liu Y, Li X, Yang P, He W. Solubilization techniques used for poorly water-soluble drugs. *Acta Pharm Sin B*. 2024;14(11):4683-716. doi: 10.1016/j.apsb.2024.08.027, PMID 39664427.
- Sha X, Yan G, Wu Y, Li J, Fang X. Effect of self-microemulsifying drug delivery systems containing Labrasol on tight junctions in Caco-2 cells. *Eur J Pharm Sci* [Internet]. 2005;24(5):477-86. doi: 10.1016/j.ejps.2005.01.001, PMID 15784337.
- Xiong G, Wu Z, Yi J, Fu L, Yang Z, Hsieh C, *et al.* ADMETlab 2.0: an integrated online platform for accurate and comprehensive predictions of ADMET properties. *Nucleic Acids Res* [Internet]. 2021;49(W1):W5-14. doi: 10.1093/nar/gkab255, PMID 33893803.
- Davis AP, Wiegers TC, Sciaky D, Barkalow F, Strong M, Wyatt B, *et al.* Comparative Toxicogenomics Database's 20th anniversary: update 2025. *Nucleic Acids Res*. 2025;53(D1):D1328-34. doi: 10.1093/nar/gkae883, PMID 39385618.
- Shamsuddin FM, Ansari SH, Ali J. Development and evaluation of solid dispersion of spironolactone using fusion method. *Int J Pharm Investig* [Internet]. 2016;6(1): 63-8. doi: 10.4103/2230-973X.176490, PMID 27014621.
- Kumar L, Suhas BS, Pai GK, Verma R. Determination of saturated solubility of naproxen using UV-visible spectrophotometer. *Res J Pharm Technol* [Internet]. 2015;8(7): 825-8. doi: 10.5958/0974-360X.2015.00134.1.

37. Jha DK, Shah DS, Talele SR, Amin PD. Correlation of two validated methods for the quantification of naringenin in its solid dispersion: HPLC and UV spectrophotometric methods. *SN Appl Sci*. 2020;2(4). doi: 10.1007/s42452-020-2536-3.
38. ICHQ RA. Stability testing of new drug substance and product and ICHQ1C stability testing of new dosage forms. *ICH quality guidelines*. In: /doi/pdf/10.1002. Vol. 1A(R2); 2017 Jan 1. An Implementation Guide [Internet] [cited Sep 25 2025];3-44. Available from: 9781118971147.ch1.
39. Remsberg CM, Yáñez JA, Vega-Villa KR, Mir ND, Andrews PK, et al. HPLC-UV analysis of phloretin in biological fluids and application to pre-clinical pharmacokinetic studies. *J Chromatogr Sep Tech* [Internet]. 2010;1(1): 1-5.
40. Borman P, elder D. In: /doi/pdf/10.1002. Vol. Q2(R1); 2017 Jan 1. Validation of Analytical Procedures. *ICH quality guidelines: An Implementation Guide* [Internet] [cited Sep 25 2025]; 127-66. Available from: 9781118971147.ch5.
41. Cen M, Liang H, Xiong X, Zeng J, Cheng X, Wang S. Development and validation of a HPLC method for determination of Isochlorogenic acid A in rat plasma and application to pharmacokinetic study. *J Chromatogr Sci*. 2017;55(10):1037-42. doi: 10.1093/chromsci/bmx072, PMID 28977404.
42. VP S, KK M, SD, IJ M, JP S, AY, et al. Analytical methods validation: bioavailability, bioequivalence and pharmacokinetic studies. Conference report. *Eur J Drug Metab Pharmacokinet* (Internet). 1991;16(4): 249-55. Available from: <https://pubmed.ncbi.nlm.nih.gov/1823867/>
43. Dudonné S, Vitrac X, Coutière P, Woillez M, Mérillon JM. Comparative study of antioxidant properties and total phenolic content of 30 plant extracts of industrial interest using DPPH, ABTS, FRAP, SOD, and ORAC assays. *J Agric Food Chem* [Internet]. 2009;57(5):1768-74. doi: 10.1021/jf803011r, PMID 19199445. Available from: /doi/pdf/10.1021/jf803011r?ref=article_openPDF.
44. Butkeviciute A, Ramanauskienė K, Janulis V. Formulation of gels and emulgels with *Malus domestica* Borkh: apple extracts and their biopharmaceutical evaluation *in vitro*. *Antioxidants* (Basel). 2022;11(2):373. doi: 10.3390/antiox11020373, PMID 35204255.
45. Deshpande RD, Shah DS, Gurrām S, Jha DK, Batabyal P, Amin PD, et al. Formulation, characterization, pharmacokinetics and antioxidant activity of phloretin oral granules. *Int J Pharm*. 2023;645:123386. doi: 10.1016/j.ijpharm.2023.123386, PMID 37678475.
46. Mizushima Y, Kobayashi M. Interaction of anti-inflammatory drugs with serum proteins, especially with some biologically active proteins. *J Pharm Pharmacol* [Internet]. 1968;20(3):169-73. doi: 10.1111/j.2042-7158.1968.tb09718.x, PMID 4385045.
47. Reshma KP, PB. *In vitro* anti-inflammatory, antioxidant and nephroprotective studies on leaves of *Aegle marmelos* and *Ocimum sanctum*. Vol. 7(4); 2014 Sep 1. *Asian Journal of Pharmaceutical and Clinical Research* [Internet]. p. 121-9 [cited Sep 25 2025]. Available from: <https://journals.innovareacademics.in/index.php/ajpcr/article/view/2735>.
48. Juvekar A, Sakat S, Wankhede S, Juvekar M, Gambhire M. Evaluation of antioxidant and anti-inflammatory activity of methanol extract of *Oxalis corniculata*. *Planta Med* [Internet]. 2009;75(09):PJ178. doi: 10.1055/s-0029-1234983.
49. Liu Z, Xiang Q, Du L, Song G, Wang Y, Liu X. The interaction of sesamol with DNA and cytotoxicity, apoptosis, and localization in HepG2 cells. *Food Chem* [Internet]. 2013; 141(1): 289-96. doi: 10.1016/j.foodchem.2013.02.105, PMID 23768360.
50. Sekhon-Loodu S, Ziaullah RHPV, Rupasinghe HP. Docosahexaenoic acid ester of phloridzin inhibit lipopolysaccharide-induced inflammation in THP-1 differentiated macrophages. *Int Immunopharmacol* [Internet]. 2015;25(1):199-206. doi: 10.1016/j.intimp.2015.01.019, PMID 25637769.
51. AMPK HDG. AMPK: Positive and negative regulation, and its role in whole-body energy homeostasis. *Curr Opin Cell Biol* [Internet]. 2015;33:1-7. doi: 10.1016/j.ccb.2014.09.004, PMID 25259783.
52. Lipinski CA, Lombardo F, Dominy BW, Feeney PJ. Experimental and computational approaches to estimate solubility and permeability in drug discovery and development settings. Vol. 23(1-3); 1997 Jan 15. *Adv Drug Deliv Rev* [Internet]. p. 3-25 [cited Sep 25 2025]. Available from: <https://www.sciencedirect.com/science/article/pii/S0169409X96004231>.
53. Monge P, Solheim E, Scheline RR. Dihydrochalcone metabolism in the rat: phloretin. *Xenobiotica* [Internet]. 1984;14(12):917-24. doi: 10.3109/00498258409151490, PMID 6531939.
54. Li B, Li R, Yan W. Solubilities of phloretin in 12 solvents at different temperatures. *J Chem Eng Data*. 2011; 56(4): 1459-62. doi: 10.1021/je101168w.
55. Crespy V, Morand C, Besson C, Manach C, Dé C, Ré C, et al. Nutrient metabolism comparison of the intestinal absorption of quercetin, phloretin and their glucosides in rats [Internet]; 2001. Available from: <https://academic.oup.com/jn/article-abstract/131/8/2109/4686963>.
56. Schmolka IR. Artificial skin. I. Preparation and properties of pluronic F-127 gels for treatment of burns. *J Biomed Mater Res* [Internet]. 1972;6(6):571-82. doi: 10.1002/jbm.820060609, PMID 4642986.
57. Akkari AC, Papini JZ, Garcia GK, Franco MK, Cavalcanti LP, Gasperini A, et al. Poloxamer 407/188 binary thermosensitive hydrogels as delivery systems for infiltrative local anesthesia: physico-chemical characterization and pharmacological evaluation. *Mater Sci Eng C Mater Biol Appl* [Internet]. 2016; 68: 299-307. doi: 10.1016/j.msec.2016.05.088, PMID 27524024.
58. Karekar P, Vyas V, Shah M, Sancheti P, Pore Y. Physicochemical investigation of the solid dispersion systems of etoricoxib with Poloxamer 188. *Pharm Dev Technol* [Internet]. 2009;14(4):373-9. doi: 10.1080/10837450802683974, PMID 19552551.
59. Bhalani DV, Nutan B, Kumar A, Singh Chandel AK. Bioavailability enhancement techniques for poorly aqueous soluble drugs and therapeutics. *Biomedicines*. 2022;10(9):2055. doi: 10.3390/biomedicines10092055, PMID 36140156.
60. Zhang J, Guo M, Luo M, Cai T. Advances in the development of amorphous solid dispersions: the role of polymeric carriers. *Asian J Pharm Sci*. 2023;18(4):100834. doi: 10.1016/j.ajps.2023.100834, PMID 37635801.
61. Sharma P, Bal T, Singh SK, Sharma N. Biodegradable polymeric nanocomposite containing phloretin for enhanced oral bioavailability and improved myocardial ischaemic recovery. *J Microencapsul* [Internet]. 2024;41(8):754-69. doi: 10.1080/02652048.2024.2418608, PMID 39431662.
62. Gu Z, Xue Y, Li S, Adu-Frimpong M, Xu Y, Yu J, et al. Design, characterization, and evaluation of diosmetin-loaded solid self-microemulsifying drug delivery system prepared by electrospray for improved bioavailability. *AAPS PharmSciTech*. 2022;23(4):106. doi: 10.1208/s12249-022-02263-3, PMID 35381887.
63. Anunciato Casarini TP, Frank LA, Pohlmann AR, Guterres SS. Dermatological applications of the flavonoid phloretin. *Eur J Pharmacol*. 2020;889:173593. doi: 10.1016/j.ejphar.2020.173593, PMID 32971088.
64. Huang S, Xu J, Peng Y, Guo M, Cai T. Facile tuning of the photoluminescence and dissolution properties of phloretin through cocrystallization. *Cryst Growth Des* [Internet]. 2019;19(12):6837-44. doi: 10.1021/acs.cgd.9b01111. Available from: /doi/pdf/10.1021/acs.cgd.9b01111?ref=article_openPDF.
65. Wang L, Li X, Mi L, Shen X, Feng T, Liu X, et al. Study on pharmacokinetics, tissue distribution, and excretion of phloretin and its prodrug 2',4',6',4-tetra-o-acetylphloretin in rats using LC-MS/MS. *Acta Chromatogr*. 2019;31(1):63-70. doi: 10.1556/1326.2017.00363.
66. Nithiya T, Udayakumar R. *In vitro* antioxidant properties of phloretin-an important phytochemical. Vol. 4(1); 2016 Jan 14. *J Biosci Med (Irvine)* [Internet]. p. 85-94 [cited Sep 26 2025]. Available from: <https://www.scirp.org/journal/paperinformation?paperid=62766>.
67. Prior RL, Hoang H, Gu L, Wu X, Bacchiocca M, Howard L, et al. Assays for hydrophilic and lipophilic Antioxidant Capacity (oxygen radical absorbance capacity (ORACFL)) of plasma and Other Biological and Food Samples. *J Agric Food Chem* [Internet]. 2003;51(11):3273-9. doi: 10.1021/jf0262256, PMID 12744654. Available from: /doi/pdf/10.1021/jf0262256?ref=article_openPDF.
68. Prior RL, Cao G, Cao G. *In vivo* total antioxidant capacity: comparison of different analytical methods. *Free Radic Biol Med*. 1999; 27(11-12): 1173-81. doi: 10.1016/S0891-5849(99)00203-8, PMID 10641708.
69. Nakamura Y, Watanabe S, Miyake N, Kohno H, Osawa T. Dihydrochalcones: evaluation as novel radical scavenging antioxidants. *J Agric Food Chem* [Internet]. 2003;51(11):3309-12. doi: 10.1021/jf0341060, PMID 12744659.
70. Rezk BM, Haenen GR, Van der Vijgh WJ, Bast A. The antioxidant activity of phloretin: the disclosure of a new antioxidant pharmacophore in flavonoids. *Biochem Biophys Res Commun* [Internet]. 2002;295(1):9-13. doi: 10.1016/S0006-291X(02)00618-6, PMID 12083758.
71. Li X, Chen B, Xie H, He Y, Zhong D, Chen D. Antioxidant structure-activity relationship analysis of five dihydrochalcones. *Molecules*. 2018;23(5):1162. doi: 10.3390/molecules23051162, PMID 29757201.
72. Li X, Liu J, Lin J, Wang T, Huang J, Lin Y, et al. Protective effects of dihydromyricetin against •OH-induced mesenchymal stem cells damage and mechanistic chemistry. *Molecules* [Internet]. 2016;21(5):604. doi: 10.3390/molecules21050604, PMID 27171068.
73. Perez CA, Wei Y, Guo M. Iron-binding and anti-Fenton properties of baicalin and baicalin. *J Inorg Biochem* [Internet]. 2009 Mar;103(3):326-32. doi: 10.1016/j.jinorgbio.2008.11.003, PMID 19108897.
74. Habtemariam S. The molecular pharmacology of phloretin: anti-inflammatory mechanisms of action. *Biomedicines*. 2023;11(1):143. doi: 10.3390/biomedicines11010143, PMID 36672652.
75. Kum H, Roh KB, Shin S, Jung K, Park D, Jung E. Evaluation of anti-acne properties of phloretin *in vitro* and *in vivo*. *Int J Cosmet Sci* [Internet]. 2016;38(1): 85-92. doi: 10.1111/ics.12263, PMID 26212527.

Cite this article: Chimthanawala NMA, Amin PD, Sathaye SS. Unmasking the Therapeutic Potential of a Bio-enhanced Phloretin Formulation: Formulation, Characterization, and Evaluation. *Indian J of Pharmaceutical Education and Research*. 2026;60(2s):s669-s686.

Table S1: Methods of optimizing the formulation

Solvent evaporation (SE)	In this method, a 1mg/ml solution was prepared by dissolving both, the drug and excipient, PHL and P188, in solvent (methanol) in a 1:1 ratio. MeOH was then allowed to evaporate and the physicochemical parameters were noted.
Melt-fusion (MF)	In a step-down fashion, 100 mg PHL was added to P188, P407 and GEL 48/16 in 03 ratios viz. 1:10, 1:20, and 1:30. In the next set, two polymers were selected i.e., P188 and GEL 48/16 in the ratios 1:5, 1:3 and 1:1 to obtain the optimum combination that offered stability.
Cold-pressed technique (CP)	100 mg PHL was dissolved in different concentrations of polymers P188 and GEL48/16 – i.e., 30%, 60%, and 90% solutions prepared in 10 ml distilled water and mixed thoroughly. After mixing, the solutions were kept overnight at cool temperature (4-8 °C) and its properties were observed after 24 hrs.